Subtopic: Alternative Fuels and Emissions

13th U. S. National Combustion Meeting
Organized by the Central States Section of the Combustion Institute
March 19–22, 2022
College Station, Texas

CFD Evaluation of Sustainable Aviation Fuel Blends for Commercial Supersonics Technology

Kumud Ajmani[1,] and Jeffrey P. Moder[2]*

[1]Engine Combustion Branch, HX5 LLC, Cleveland OH, USA
[2]Engine Combustion Branch, NASA Glenn Research Center, Cleveland OH, USA
**Corresponding Author Email: kumud.ajmani-1@nasa.gov*

Abstract: An overview is provided of a CFD study on the impacts of fuel blends on NOx emissions and flame structure in an axially staged combustor operating at a supersonic cruise condition. The Open version of the National Combustion Code (OpenNCC) was used to perform two-phase reacting flow computations with various blending ratios of an 'average' Jet-A (A2) and Gevo Alcohol-to-Jet (C1) for RTRC's Axially Controlled Stoichiometry (ACS) combustor. The predicted flame structures in the ACS combustor with three different blending ratios of the A2 and C1 fuel were very similar. The predicted NOx emissions for all fuel blends were within 10% of the experimentally measured range of NOx emissions for 100% A2 fuel.

Keywords: Gas Turbine Combustion, Fuels, Computational Fluid Dynamics

1.0 Introduction

In efforts to mitigate the future impacts of using fossil-based aviation fuels on the environment, the aerospace community is investing significant resources into using Sustainable Aviation Fuels (SAFs) in liquid-fueled gas-turbine combustors [1, 2]. Future commercial supersonic aircraft are likely to use high blends of SAF or 100% SAF to reduce life-cycle carbon emissions. Reducing emissions that impact the environment and human health is a significant research area under NASA's Commercial Supersonic Transport (CST) project. This effort assessed the impact of Jet-A/SAF fuel blends on NOx emissions and flame structure for an axially staged combustor operating at a supersonic cruise condition.

The average Jet-A fuel (A2) and the Gevo Alcohol-To-Jet fuel (C1) characterized and tested under the Nation Jet Fuel Combustion Program [2] were used as the two blending components for this study. The combustor used for this study was the Axially Controlled Stoichiometry (ACS) combustor designed and tested under NASA's Environmentally Responsible Aviation (ERA) and Advanced Air Transport Technology (AATT) programs [3] by Pratt & Whitney/RTRC [4]. While this combustor was not optimized for a supersonic aircraft cycle, it provided a realistic low-NOx combustor design for an initial assessment of fuel impacts on NOx emissions at supersonic cruise conditions. Commercial supersonic aircraft will spend most of their flight envelope at cruise, at high combustor operating temperatures. The combination of higher operating temperature for longer flight periods, combined with the goal of ultra-low NOx emissions at cruise, creates unique design challenges for thermal management and emissions at cruise for CST aircraft combustors [5]. The current CFD evaluation is a follow-on study from previous work which had evaluated the emissions and flame-structure of the ACS combustor for three different, unblended fuels: 'average' Jet-A (A2), RP-2 and SASOL iso-paraffin kerosene (IPK) [6].

The first step of the CFD study verified the multi-component lagrangian spray modeling approach [7] and an 81-species skeletal-kinetics mechanism implementation [8] for blends of A2 and C1 fuels within the OpenNCC code. The second step of the study used OpenNCC to evaluate the ACS combustor for three arbitrary blending ratios of A2 and C1 fuels consisting of 80% A2 and 20% C1, 50% A2 and 50% C1, and 20% A2 and 80% C1, respectively. The aerodynamics and flame characteristics predicted by OpenNCC for the ACS combustor were compared for all fuel blends, and the predicted emissions (EINOx, EICO) for all blends were compared with the available experimental data for 100% Jet-A.

2.0 ACS Combustor Flametube Design

Figure 1 shows a section of RTRC's combustor designed to meet performance and emissions requirements for subsonic aviation under NASA's N+3 Advanced Air Transport Technology (AATT) program. RTRC's design is based on an axially staged lean burn approach and is referred to as ACS (Axially Controlled Stoichiometry). The fuel flow conditions of the Pilot and Main stages can be independently controlled for various flight conditions. The combustor section was instrumented and tested to obtain emissions and performance data at various N+3 subsonic cycle conditions at NASA Glenn Research Center. Emissions data (EICO, EINOx) was also obtained for certain operating points (cruise, maximum power) corresponding to a NASA Supersonic Cycle designed for CST applications. The nominal cruise conditions for this NASA engine cycle were P_3=15.9bar (234psi), T_3=884K (1132F), equivalence ratio (phi)=0.39 (Fuel-Air Ratio, FAR=0.0267) and combustor pressure-drop, Δp=3.46% [4].

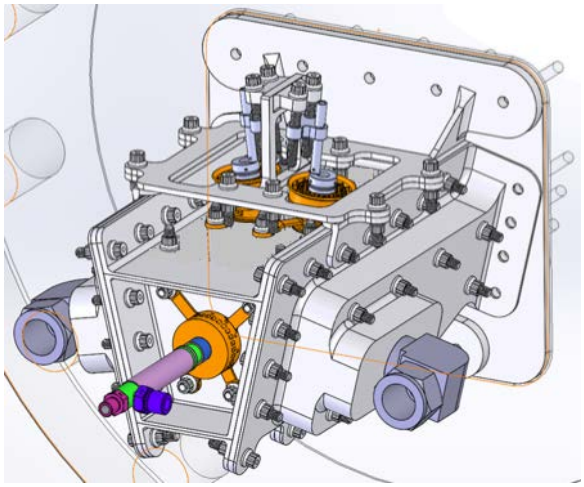

Figure 1. Sector layout of ACS Combustor (RTRC / P&W) as tested at NASA GRC

3.0 CFD Evaluation of Arbitrary Fuel Blends for ACS Combustor at Supersonic Cruise

This paper reports OpenNCC computations at supersonics cruise conditions for RTRC's ACS flametube array developed to minimize EINOx emissions for NASA's N+3 program. The ACS configuration underwent performance and emissions testing at NASA Glenn Research Center's CE-5 medium pressure facility. A lagrangian-spray modeling (for the liquid phase droplets) [7] and a finite-rate reduced-kinetics mechanism [8] were used within OpenNCC CFD to compute heat release, flame-structure, and emissions. Reacting flow simulations were performed for two different fuels with varying compositions (see Table 1), blended in varying ratios from 100% A2 to 20% A2. The initial computations were performed to establish 'baseline' combustor performance and emissions with 100% A2 fuel. These computations were followed by a CFD comparison of flame-structure and emissions between blends of 80% A2 and 20% C1 (80/20), 50% A2 and 50% C1 (50/50), and 20% A2 and 80% C1 (20/80), respectively.

Gevo ATJ (Alcohol-to-Jet or C1) was chosen as the Sustainable Aviation Fuel (SAF) for this study for three reasons: (a) C1 is composed primarily of long, branched chain iso-paraffins, and has a much

higher ignition-delay as compared to A2 fuel [2]. This makes it potentially useful as a candidate to be blended with A2 to help reduce the thermal load on the combustor dome at supersonic cruise conditions. (b) C1 can be produced by synthetic processes, which makes it a candidate to be a Sustainable Aviation Fuel (SAF) for aviation applications. (c) A reduced finite-rate kinetics model [8] of 81 species were readily available for CFD evaluation of the various blends of A2 and C1 fuel.

Table 1. Compositions of three different fuels evaluated with OpenNCC for the ACS Combustor

Fuel Composition	'Average' Jet-A (A2)	Gevo ATJ (C1)
aromatics	20%	1%
iso-paraffin	20%	99%
n-paraffin	20%	0%
cyclo-paraffin	40%	0%

3.1 Chemical Kinetics Modeling for A2 and C1 Fuels

A modeling approach using two CANTERA [9] models, one for flame-speed and flame-temperature calculations, and the other for computing ignition-delay, was used to perform quick validation checks of a HyChem skeletal kinetics model [8] for various blending ratios of A2 and C1 fuels. The CANTERA computations served as a quick validation exercise before the kinetics model were implemented for extensive, 3-D reacting flow computations with the OpenNCC CFD code. Some details of the chemical and combustion properties of A2 and C1 fuels, as used in the HyChem kinetics modeling, are shown in Table 2. All gas-phase thermodynamic and transport properties used for both the CANTERA and OpenNCC modeling were those that accompanied the HyChem skeletal kinetics mechanism [8]. In general, a skeletal kinetics approach greatly reduces computational times for CFD as compared to a detailed kinetics approach. This is partly attributed to reduced numerical stiffness and lower number of species of a skeletal kinetics mechanism.

Table 2. Chemical properties and kinetics of A2 and C1 fuels evaluated with OpenNCC

Fuel Property / Kinetics [8]	A2	C1
Chemical Formula (Average)	$C_{11.4}H_{21.7}$	$C_{12.5}H_{27.1}$
H/C ratio	1.90	2.16
Derived Cetane Number (DCN)	47	16
Net heat of Combustion (MJ/kg)	42.8	43.9
Chemical Formula (Modeled)	$C_{11}H_{22}$	$C_{13}H_{28}$
Number of Species (Skeletal Kinetics)	51	51
Species for NOx Kinetics	30	30

The baseline skeletal kinetics mechanism for modeling arbitrary blends of A2 and C1 fuels consists of 51 species, with an additional 30 species to account for NOx related computations. The CANTERA computed values for flame temperature, ignition delay and flame speed as performed for a supersonic cruise cycle condition of interest in this work (P_3= 15.9bar, T_3=884K, phi=0.39), are shown in Table 3. As expected, the computed flame temperature for both fuels is virtually identical. The computed flame speed for 100% A2 is 10% higher than that for 100% C1, which is consistent with experimental results [8].

The computed ignition delay time (IDT) for 100% C1 is 10% lower than that for 100% C1, which is also consistent with experimental results [8] which showed that the IDT of both A2 and C1 are dependent on temperature. At the computed temperature of T_3=884K, i.e., T_3<1250K, the IDT is controlled by the rate of fuel decomposition, in contrast to being controlled by the rate of oxidation of the decomposed products when T_3>1250K. Experimental results showed that C1 decomposes faster than A2 at T_3=884K, which leads to a lower induction time and correspondingly lower IDT for C1 as compared to A2. The experimental

behavior of a lower IDT for 100% C1 fuel as compared to 100% A2 fuel at T_3<1250K, was correctly predicted by the CANTERA computations. Table 3 also shows results for CANTERA computations for the three fuel blends used in the OpenNCC 3-D CFD analysis, i.e., 80/20, 50/50 and 20/80 volumetric ratios of A2 and C1, respectively. As expected, the results for all the three computed blending ratios of A2 and C1 are bounded by the results for the 100% A2 and 100% C1 fuels.

Table 3. Combustion characteristics of A2 and C1 at P_3=15.9bar, T_3=884K, phi=0.39 (CANTERA computations)

Combustion Characteristic	100% A2	80% A2 20% C1	50% A2 50% C1	20% A2 80% C1	100% C1
Adiabatic Flame Temperature, K	1780.9	1781.5	1782.3	1782.9	1783.3
Ignition Delay Time, ms	24.9	21.4	18.6	19.1	22.4
Flame Speed, cm/s	32.6	32.1	31.7	30.8	30.2

3.2 Spray Modeling and Liquid Properties for A2 and C1 Fuels

The skeletal finite-rate kinetics models for the two fuels, A2 and C1, were coupled with OpenNCC's lagrangian-spray liquid-fuel modeling to compute heat release, flame-structure, and emissions for the ACS combustor. The pressure-atomizing circuit of the Pilot was modeled as a single hollow cone injector with 16 streams, and the six jet-in-crossflow injectors of the second Pilot circuit were each modeled as a solid cone injector with 2 injection streams. Each injection stream provided stochastic variations of injection angle and velocity for the spray simulation. Each of the six fuel inlets of the two high-shear injectors (Mains) were also modeled as a solid cone injector with 2 streams. The droplet size distribution for injected particles was prescribed by the correlation equation:

$$\frac{\delta n}{n} = 4.21 \times 10^6 \left[\frac{d}{d_{32}}\right]^{3.5} e^{-16.98\left[\frac{d}{d_{32}}\right]^{0.4}} \frac{\delta d}{d_{32}} \quad (1)$$

Here n is the total number of droplets, d_{32} is the Sauter mean diameter (SMD), and δn is the number of droplets in the size range between d and $d + \delta d$. In this work, each CFD 'injector' used eight droplet 'groups' to provide droplet size variations based on the correlation of Eq. 1. The modeling choices of 16 streams for the pressure atomizer, and 2 streams for each of the 18 jet-in-cross flow 'holes', combined with 8 droplet size groups for all injectors, resulted in 704 new liquid particles introduced into the CFD domain at each injection time-step.

Table 4. Physical properties of A2 and C1 for liquid-phase modeling with OpenNCC

Liquid Fuel Property	A2	C1
Molecular Weight (g/g-mole)	154.1	184.3
Normal Boiling Point (K)	489.5	459.0
Density at 1bar (kg/m^3)	791.5	748.0
Critical Temperature (K)	760.4	740.2
Critical Pressure (bar)	18.2	18.0
Heat of Vaporization (kJ/kg)	310.0	256.3
Critical Volume (cm^3/g-mole)	700.4	713.0

The liquid physical properties used for the spray-modeling of A2 and C1 in the current work are listed in Table 4. In this study, the temperature-dependent liquid properties (density, heat capacity, viscosity, vapor pressure, latent heat) for A2 and C1 fuels were implemented from the work of Esclapez [10]. In addition, an extensive effort was undertaken to (a) verify that OpenNCC's evaporation model [7] accurately predicted the differential evaporation effects of the A2 and C1 fuels, and (b) verify that the primary

pyrolysis species of C_2H_4 and iC_4H_8 for A2 and C1, respectively, were accurately modeled by OpenNCC for the various blending ratios of A2 and C1 by the skeletal kinetics [8] chosen for this study. Detailed results for these validation studies of differential evaporation modeling and species production will be presented in a future paper.

3.3 OpenNCC Simulation Procedure for Blends of A2 and C1 Fuels

Four sets of tetrahedral meshes of increasing mesh densities were generated for the ACS Combustor with LLNL's CUBIT mesh generation software [11]. Non-reacting solutions were computed with OpenNCC for each mesh and the predicted 'effective area' (ACd) for the Pilot injector and the Main injectors were compared with experimental data. The final mesh had a less than 10% error between the predicted and measured ACd values for the combustor and consisted of 24.4 million tetrahedral elements and 4.3 million nodes.

The OpenNCC CFD computations for all fuel blends of A2 and C1 were performed for a supersonic cruise condition of P_3=15.9bar (234psi), T_3=884K (1132F), phi=0.39 (FAR=0.0267) and Δp=3.46%. The inlet boundaries for the Pilot and Main injectors were modeled with fixed total pressure and total temperature conditions derived from the P_3 and T_3 for the cruise condition. The outflow boundary was modeled with a fixed static-pressure for subsonic outflow based on the specified Δp between the inflow and outflow of the combustor. No-slip, adiabatic flow conditions were imposed at all solid surfaces. The cooling-hole flows at the three walls: combustor dome, upper wall, and lower wall, were modeled with a wall-injection boundary condition. The fuel-flow boundary conditions used the experimentally specified liquid fuel flows to fix the fuel flow rate for the Pilot (two circuits) and both the Main injectors. The percentage share of A2 and C1 fuel for each fuel-blend was modeled by specifying the mass-fraction component of each fuel at the injector inlets.

The initial conditions for the CFD computations represented static air at P_3 and T_3 in the entire computational domain. RANS CFD with a 2^{nd}-order accurate central-differencing operator and 4-stage explicit Runge-Kutta time-integration was used to establish a converged non-reacting flow-field. The non-reacting RANS solution was then used to generate a time-accurate solution using a dual-time stepping approach, coupled with the Time-Filtered Navier Stokes (TFNS) solver of OpenNCC. The physical time-step was set to 1e-6s, and 10000 time-steps were computed to obtain the non-reacting TFNS solution. A reacting-flow TFNS computations (51species, without NOx chemistry) was then obtained, with initiation of fuel-injection and two-phase computations, and artificial ignition of the fuel-air mixture downstream of each of the injectors. Complete details of the OpenNCC's numerical and turbulence models, and the finite-rate chemistry solvers are available in [5].

The reacting-flow solutions for each fuel blend were considered converged when the variation in the area-averaged values of temperature, CO, and gas-phase FAR at the combustor exit were within 5% over successive flow-through cycles. Liquid phase convergence was achieved when the mass-imbalance between injected and evaporated fuel was below 1% of the total injected fuel mass. The liquid-phase solution typically converged at least an order of magnitude faster in physical times, as compared to the gas-phase area-averaged quantities. Reacting flow solutions with an 81-species skeletal mechanism (30-species NOx kinetics) were then initiated, and converged solutions for EINOx were obtained for each fuel blend. At least five additional flow-through cycles were required to meet the EINOx convergence criteria of < 5% variation in exit-plane area-averaged NO between successive flow cycles.

All computations were performed on 50 nodes (Intel Ivy-Bridge, 20 cores/node) of NASA's Advanced Supercomputing (NAS) Pleiades cluster. Each reacting flow solution (without NOx) required approximately 1200 wall-clock hours. The NOx-enabled kinetics computations required an additional 3600 wall-clock hours for each fuel blend computation. The CFD results were post-processed with VisIt [12] to produce contour plots at several cross-sections of the ACS combustor (see figure 2). The sections AA and BB are across the vertical centerline (YZ plane) and the horizontal centerline (XZ plane) of the pilot injector, respectively. Section CC is across the vertical centerline (XY plane) of the two downstream main injectors. CFD predictions at sections AA, BB and CC were chosen as they represent some of the key aerodynamic and reacting flow features of the ACS combustor. Due to the proprietary nature of the

P&W/RTRC combustor design, some details of the Pilot and Main injectors have been removed from the CFD results shown for the three cross-sections.

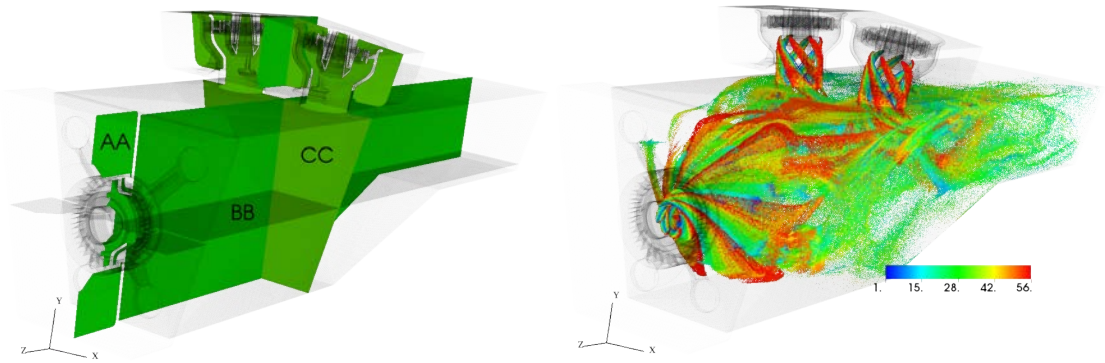

Figure 2. Cross-Sections of ACS Combustor chosen for comparisons of CFD results (left); Typical spray particle distribution for reacting flow CFD (right), colored by particle diameter (μm)

3.4 OpenNCC CFD Predictions: Axial Velocity and Temperature Profiles

Figure 3 shows a comparison of the axial velocity contours (reacting flow) for the three fuel blends (80%, 50%, 20% A2) at three cross-sections of the combustor. As expected, the aerodynamic features for all the three fuels are very similar to each other. Sections AA and BB show that the recirculation zone near the combustor dome is virtually identical for all three fuels. Section AA shows a significant acceleration in the flow, particularly near the center of the flowfield. This acceleration is due to the mixing of the flow from the main injector streams with the pilot stream in the vicinity of the area reduction created by the bottom ramp of the combustor. Sections CC shows strong vertical penetration (blue regions) and mixing of the center-jets of the two main injectors with the axial flow (green regions).

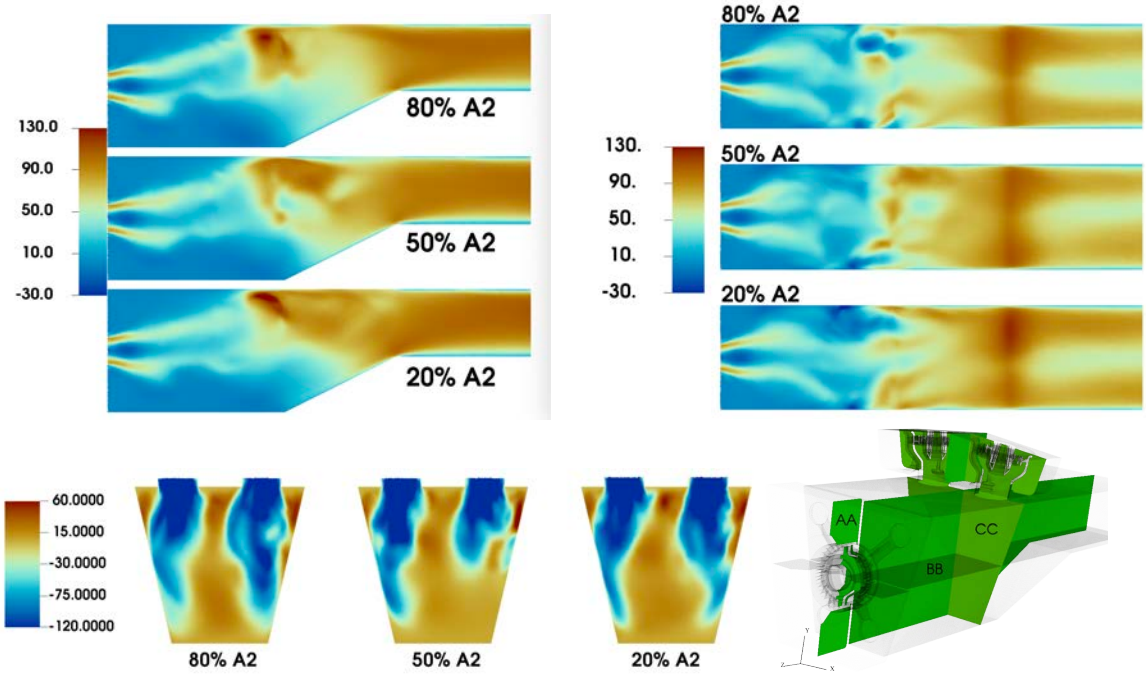

Figure 3. Velocity (m/s) contours at section AA (top, left), BB (top, right) and CC (bottom, left)

Figure 4 shows a comparison of the temperature contours for the three fuel blends (80%, 50%, 20% A2) at three cross-sections of the combustor. The flame-shape and size for the for all three cases, both downstream of the pilot injector (section AA, BB), and in the center-plane of the two main injectors (section CC) were very similar to each other. The similarities in the flame structures and the relative

strengths of the three flames as indicated by the locations of the peak temperatures in the flames are consistent with the very similar ignition delay times and flame speeds for the three fuel blend ratios (see section 3.1, Table 2). The CFD predictions with OpenNCC thus suggest that there are no significant effects on flame location, flame structure and flame stability when using arbitrary blends of A2 and C1 fuels at supersonic cruise conditions in the ACS combustor.

A significant portion of the primary axial flow is constricted by the vertical down-flow of the main injectors, which creates poor mixing and temperature variations in the region downstream of the location of the two main injectors in the combustor (converging ramp region in Figure 4, sections AA and BB). The OpenNCC CFD prediction of high 'mixedness' of the axial and vertical streams in the ramp region of the combustor particularly affects the CO emissions predictions, as will be discussed in the next section.

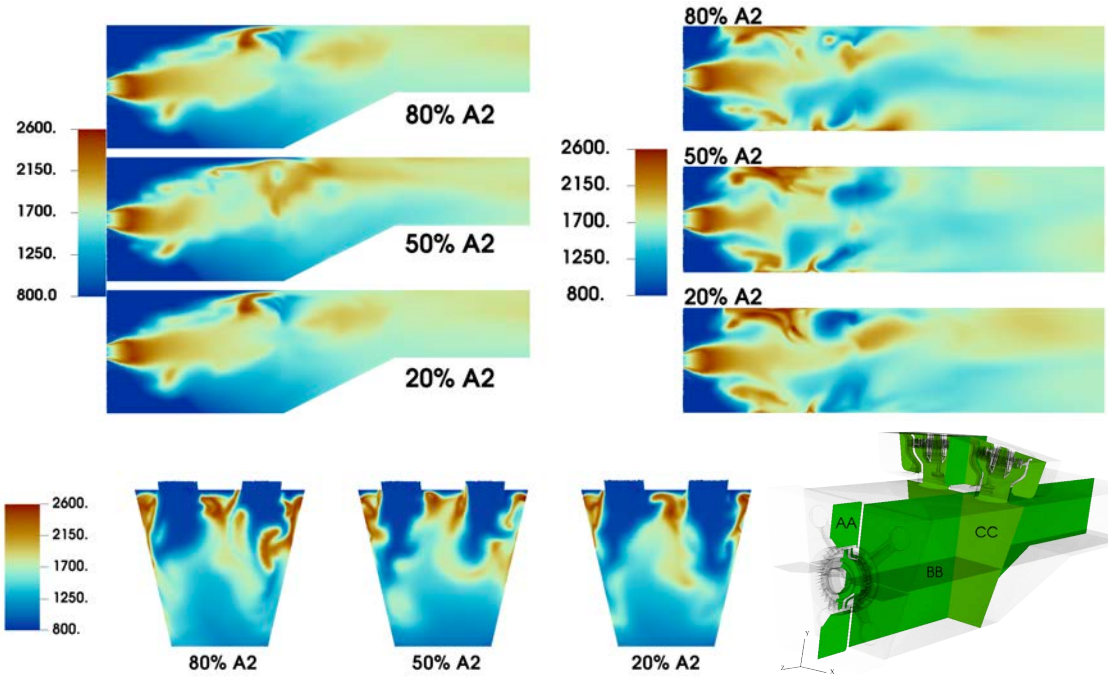

Figure 4. Temperature (K) contours at section AA (top, left), BB (top, right) and CC (bottom, left) at CST Cruise conditions

3.5 OpenNCC CFD Predictions: NO and CO mass-fractions

One primary goal of the current CFD effort was to evaluate the differences in NOx and CO emissions for the blending ratios of A2 and C1 at supersonic flight conditions. This section describes the qualitative differences in emissions for the three blending ratios, as shown in Figures 5 and 6, for NO and CO, respectively. The NO mass-fraction contours show that the NO production for the 80% and 20% A2 blends is slightly higher near the combustor dome in the region near the Pilot injector located at the combustor dome (left end of sections AA and BB). The NOx production in the cross-sectional plane of the two main injectors (section CC) is similar for all three blends. The net effect of these small differences in the NOx production is that the total NOx, as computed at the exit plane of the ACS combustor is very similar for all three blend ratios . The CFD predicted EINOx (g of NO per kg of fuel) values for the three blend ratios are 15.5 (80% A2), 14.5 (50% A2) and 16.0 (20% A2), respectively. The computed EINOx for all three blending ratios are within 10-20% of the computed EINOx for 100% A2 fuel (18.5), and within 10% of the lower end of the measured range of EINOx (18.0 +/- 3.2) for 100% A2 fuel. The CFD predictions suggest that the blending of A2 and C1 could reduce NOx emissions for the ACS combustor at supersonic cruise conditions. Future experimental testing with A2 and C1 blends could help verify these CFD predictions of lower EINOx for the ACS combustor.

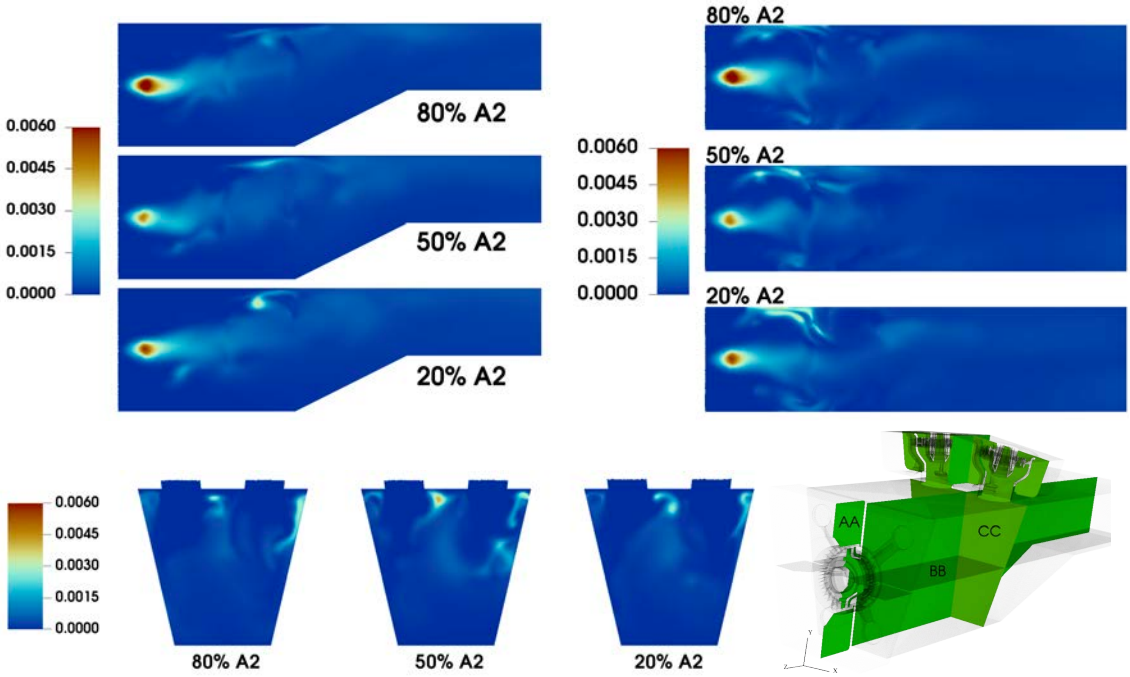

Figure 5. NO mass-fraction contours for three blends at section AA (top, left), BB (top, right) and CC (bottom, left)

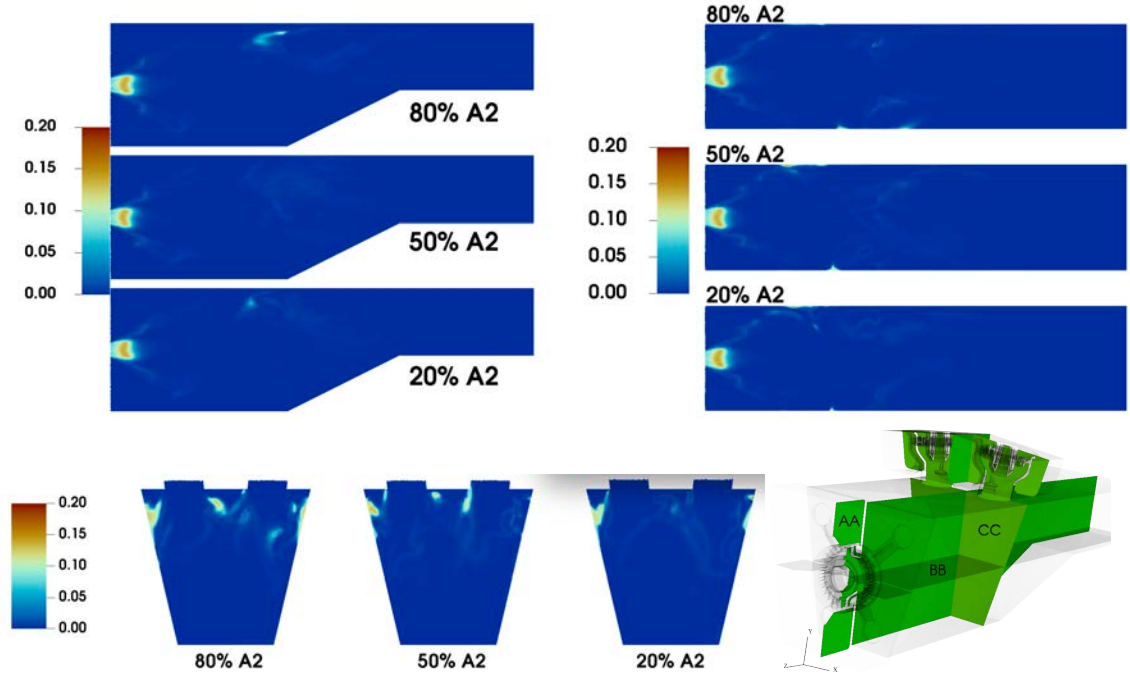

Figure 6. CO mass-fractions for three blends at section AA (top left), BB (top, right) and CC (bottom, left)

The predicted CO mass-fractions for the fuel blends studied in the current work are shown in figure 6. The production of CO in liquid-fueled combustors is primarily influenced by fuel vaporization, fuel-air mixing, and the pyrolysis process of the fuel. The current CFD computations used an identical spray-modeling and chemical-kinetics approach for all fuel blends evaluated in this study (see sections 3.1 and 3.2). Figure 6 shows that there are some very minor differences in the CO contours for the three blend ratios in the various cross-sections. The CFD predicted EICO (g of CO per kg of fuel) values for the three blend ratios are 3.9 (80% A2), 4.1 (50% A2) and 4.0 (20% A2), respectively. All three values of EICO for the A2 and C1 blends are within 10% of the computed EICO of 4.5 for 100% A2 fuel. The OpenNCC

EICO predictions are higher than the experimental value of 1.5, which can be partly attributed to the need for better modeling and resolution of fuel evaporation and fuel-air mixing, particularly for the two high-shear main injectors. The EICO predictions in the current work are consistent with those reported previously with 100% A2 fuel for the ACS Combustor [6].

A summary of comparisons of CFD predictions of EINOx (g of NOx per kg of fuel), EICO (g of CO per kg of fuel) and T_4 (exit temperature) for the different fuel blends are shown in Table 5. All CFD results are area-averaged values of the respective quantities at the combustor exit plane. The experimentally measured values of EINOx and EICO for the 100% A2 fuel are also included, for comparison with the CFD predictions. The emissions results shown in Table 5 can be summarized as below:

1. CFD predictions of NOx emissions for all three fuel blend mixtures are within 10% of each other at CST Cruise conditions.
2. CFD predictions of NOx emissions for all three fuel blend mixtures are within 10% of the lower end of the range of measured experimental values for 100% A2 fuel at CST Cruise conditions.
3. CFD predictions of CO emissions for all three fuel blend mixtures are similar to each other, and higher than experimental values for 100% A2 fuel at CST Cruise conditions.

Table 5. Comparisons of EINOx, EICO and Flame Temperature (T_4) for various fuel blends of A2 and C1 fuels with experimental data at supersonics cruise (P_3= 15.9bar (234psi), T_3=884K (1132F), phi=0.39). Fuel blending is by %volume.

A2 %	C1 %	EINOx	EICO	T_4 (K)
100 (Experiment)	0	18 +/- 3.2	1.5	1781
100	0	18.5	4.5	1780
80	20	15.5	3.9	1785
50	50	14.5	4.1	1783
20	80	16.0	4.0	1780

4.0 Summary and Significance

The impacts of blending 'average' Jet-A (A2) and a sustainable aviation fuel, Gevo ATJ (Alcohol-to-Jet or C1) on flame structure and emissions at supersonic cruise conditions were successfully modeled with the OpenNCC code. The current work examined three blend ratios of A2 and C1 fuels and demonstrated the capability to perform eddy-resolving CFD simulations including NOx chemistry for arbitrary fuel blends. The fuel blends studied captured a large range of variation in composition and combustion properties. The CFD results predicted only small variations in flame characteristics and NOx emissions for A2/C1 fuel blends ranging from 100% A2 to 20% A2/80% C1 burning in a next-generation axially-staged combustor operating at a supersonic-cruise stable-flame condition.

5.0 Acknowledgements

This research was funded by the Commercial Supersonics Technology (CST) Project under NASA's Advanced Air Vehicles Project (AAVP). Computational resources were provided by the NAS Supercomputing at NASA Ames Research Center.

6.0 References

[1] Colket, M., Heyne, J. editors, "*Fuel effects on operability of aircraft gas turbine combustors,*" AIAA, https://doi.org/10.2514/4.106040, 2021.

[2] Edwards, T., "Reference Jet Fuels for Combustion Testing," AIAA SciTech Forum, Grapevine, Texas, 55th AIAA Aerospace Sciences Meeting. AIAA Paper 2017-0146. https://doi.org/10.2514/6.2017-0146

[3] Zhuohui J. He, Tyler G. Capil, Clarence Chang Derek Podboy, and Lance L. Smith, "Emission Characteristics of an Axially Staged Sector Combustor for a Small Core High OPR Subsonic Aircraft Engine," NASA NTRS Report 20200000355, January 2020. https://ntrs.nasa.gov/citations/20200000355.

[4] Lance L. Smith, "Fuel Flexible Combustor for High-OPR Compact-Core N+3 Propulsion Engine," NASA NTRS Report 20200001621, March 2020. https://ntrs.nasa.gov/citations/20200001621.

[5] Ajmani, K., Lee, P., Chang, C.T. and Kudlac, M.T., "CFD Evaluation of Lean-Direct Injection Combustors for Commercial Supersonics Technology," AIAA Paper 2019-4199, AIAA Propulsion and Energy Conference 2019, July 2019, Indianapolis IN.

[6] Ajmani, K., and Chang, C.T., "CFD Evaluation of Aviation Fuels for Commercial Supersonics Technology," AIAA Paper 2022-1105, AIAA Scitech Meeting 2022, January 2022, San Diego CA.

[7] M.S. Raju, "LSPRAY-IV: A Lagrangian Spray Module," NASA CR-2012-217294.

[8] K. Wang, R. Xu, T. Parise, J. Shao, A. Movaghar, D.J. Lee, J. Park, Y. Gao, T. Lu, F.N. Egolfopoulos, D.F. Davidson, R.K. Hanson, C.T. Bowman, H. Wang, "A physics-based approach to modeling real-fuel combustion chemistry - IV. HyChem Modeling of Combustion Kinetics of a Bio-derived Jet Fuel and its Blends with a Conventional Jet A," *Combustion and Flame* 198 (2018) 477–489.

[9] David G. Goodwin, Harry K. Moffat, Ingmar Schoegl, Raymond L. Speth, and Bryan W. Weber. *Cantera: An object-oriented software toolkit for chemical kinetics, thermodynamics, and transport processes*. https://www.cantera.org, 2022. Version 2.6.0. doi:10.5281/zenodo.6387882

[10] Lucas Esclapez, Peter C. Ma, Eric Mayhew, Rui Xu, Scott Stouffer, Tonghun Lee, Hai Wang, Matthias Ihme, "Fuel effects on lean blow-out in a realistic gas turbine combustor," *Combustion and Flame*, 181 (2017). https://dx.doi.org/10.1016/j.combustflame.2017.02.035

[11] Teddy D. Blacker, Steven J. Owen, Matthew L. Staten, William R. Quadros, Byron Hanks, Brett W. Clark, Ray J. Meyers, Corey Ernst, Karl Merkley, Randy Morris, Corey McBride, Clinton Stimpson, Michael Plooster, and Sam Showman. *CUBIT Geometry and Mesh Generation Toolkit 15.2 User Documentation*. United States: N. p., 2016. Web. https://doi.org/10.2172/1457612

[12] Hank Childs, Eric Brugger, Brad Whitlock, Jeremy Meredith, Sean Ahern, David Pugmire, Kathleen Biagas, Mark Miller, Cyrus Harrison, Gunther H. Weber, Hari Krishnan, Thomas Fogal, Allen Sanderson, Christoph Garth, E. Wes Bethel, David Camp, Oliver Rubel, Marc Durant, Jean M. Favre, and Paul Navr, "VisIt: An End-User Tool for Visualizing and Analyzing Very Large Data," *High Performance Visualization--Enabling Extreme-Scale Scientific Insight (2012), 357-372.*